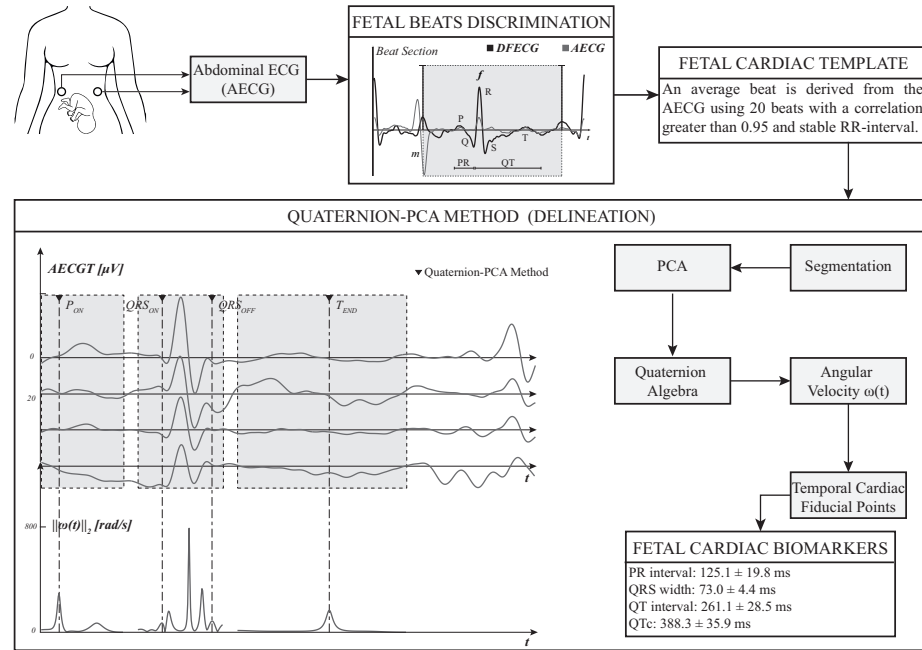


Graphical Abstract

An approach to compute Fetal Cardiac Biomarkers from the Abdominal Electrocardiogram



Highlights

An approach to compute Fetal Cardiac Biomarkers from the Abdominal Electrocardiogram

- Fetal biomarkers are obtained from non-invasive abdominal ECG.
- A novel averaging technique is developed to obtain high-correlated fetal beats.
- Onset and end of fetal cardiac waves are computed by using PCA and quaternions.

An approach to compute Fetal Cardiac Biomarkers from the Abdominal Electrocardiogram

Abstract

Objective: The fetal electrocardiogram (FECG) can be recorded from the 20th week of gestation. The aim of this work is to determine fetal cardiac biomarkers from non-invasive cardiac signals that may be useful in the assessment of fetal health. **Methods:** We have developed an algorithm to obtain FECG fiducial points. It started by discriminating fetal heartbeats based on the relative location between fetal and maternal QRS complexes. An average beat is derived from the Abdominal Electrocardiogram (AECG) using 20 beats with a correlation greater than 0.95 and stable RR-interval, based on data from 12 fetuses (38th-42nd weeks). We have implemented a combination between quaternion algebra and principal component analysis (Q-PCA method) to determine the onset and end of FECG waves by analyzing the angular velocity of the heart electrical vector. To validate our findings, we compared them with measurements obtained from the Direct Fetal Electrocardiogram (DFECG), as a benchmark. **Results:** The values calculated by the Q-PCA method and their correlation with the DFECG were as follows: PR interval: 125.1 ± 19.8 ms ($\rho = 0.97$, p-value < $2.39e - 7$), QRS duration: 73.0 ± 4.4 ms ($\rho = 0.67$, p-value < $1.74e - 2$), QT interval: 261.1 ± 28.5 ms ($\rho = 0.84$, p-value < $7.05e - 4$) and QTc interval: 388.3 ± 35.9 ms ($\rho = 0.79$, p-value < $2.27e - 3$). **Conclusion:** Given its importance and the measurement performance achieved, the methodology presented represents a significant potential tool for improving the diagnosis of fetal health.

Keywords: Non-Invasive Fetal Electrocardiogram, Principal Component Analysis, Quaternion

1. Abbreviations

- AECG: Abdominal electrocardiogram
- DFECG: Direct fetal electrocardiogram
- ECG: Electrocardiogram
- FHR: Fetal heart rate
- MECCG: Maternal electrocardiogram
- AECGT: Abdominal electrocardiogram template
- DFECGT: Direct fetal electrocardiogram template
- FECG: Fetal electrocardiogram
- GA: Gestational age
- NIFECG: Non-invasive fetal electrocardiogram

2. Introduction

During several stages of pregnancy, the health and growth of the fetus are monitored, mainly using ultrasound as a medical technology for prenatal control [1]. Heart monitoring technologies, such as cardiotocography and ultrasound, can detect complications that directly or indirectly affect the cardiovascular system. This is achieved, for example, through the measurement of fetal heart rate (FHR). However, a study suggested that FHR parameter as a diagnostic pattern did not reduce fetal morbidity or mortality, on the contrary, it increased gradually the use of cesareans, forceps, and vacuum-assisted delivery [1, 2, 3]. Kahankova et. al [4], explained that with cardiotocography introduction the perinatal mortality rate decreased but it has not suffered a significant decrease in the last 30 years. Additionally, certain heart conditions cannot be identified using these techniques since they only measure the heart rate overlooking all the additional information that an electrocardiogram could provide [1].

In advanced stages of pregnancy, the fetal electrocardiogram (FECG) can be recorded by non-invasive fetal electrocardiogram (NIFECG) using electrodes placed on the maternal abdominal surface, also call abdominal electrocardiogram (AECG). It is also possible to record by direct fetal electrocardiography (DFECG) using electrodes placed on the fetal scalp, which is invasive and can only be done during labour. AECG is composed of maternal and fetal cardiac electrical signals plus several noises, such as maternal electromyographic activity, and equipment interference, among others. In addition, AECG allows us to get a more accurate estimate of FHR and fetal health information from temporal cardiac indices [5]. One difficulty in obtaining the fetal signal is that it is at least ten times smaller than the maternal signal [3, 5, 6, 7]. The difference may be more pronounced in the early stages of pregnancy. In addition, the two signals share a large part of the frequency spectrum [2, 3].

As in the present work, several authors have implemented a variety of processing techniques to obtain fetal cardiac biomarkers [8, 9, 10, 11]. Also, the state of the art shows that FECG can be used to identify fetal hypoxia, acidosis and various arrhythmias, among others [5, 12, 13, 14]. A prolonged QT interval is indicative of fetal heart risk [1] related to different malignant arrhythmia [15]. Abnormalities in cardiac repolarization can be identified from the T-wave morphology allowing the prevention of serious cardiovascular disease [16, 17]. The PR and QRS fetal intervals normally lengthen and increase in parallel with the weight gain of the fetal heart and the mass of the ventricles during pregnancy [18]. However, abnormal alterations in ECG interval duration are also associated with illness, either hypertrophy or hypoplasia. Likewise, if these parameters do not increase as pregnancy progresses, this may also indicate fetal

growth restrictions [3, 18]. It is important to note that the use of fetal biomarkers for early diagnosis is still being researched.

This study aims to develop a non-invasive method to calculate fetal biomarkers used in the clinical practice from AECG, such as the PR interval, QT interval, QTc, and QRS complex duration. The process begins with the discrimination and selection of fetal beats to generate beat templates. Templates are used to reduce the influence of noise on the identification of cardiac waves fiducial points. Previously, we have already observed that at the onset and end of each wave, there are large deflections of the angular velocity of the cardiac electrical vector [19, 20, 21]. Therefore, we identify the fiducial points based on the angular velocity calculated from principal component analysis and quaternion algebra.

3. Materials and methods

3.1. Database

We used *Abdominal and Direct Fetal ECG database* [22, 23], which was integrated by multichannel recordings, 5 minutes each, of 12 patients collected by *The Department of Obstetrics and Gynecology of the Medical University of Silesia in Katowice, Poland*. Ethical approval was obtained from University Bioethics Committee (Commission approval number NN-013-345/02) [22, 23]. The database includes signals recorded during labor between the 38th and 42nd weeks of gestation. It was measured with a parallel recorder of AECG and DFECG. The fetal heart electrical activity was recorded with the developed KOMPOREL system, which amplified the signals with a low noise level (below $1\mu V$) and a high Common Mode Rejection Ratio of 115 dB. Four AECG electrodes were placed around the navel, one reference electrode was placed above the pubic symphysis, and one common mode reference electrode (with active-ground signal) was placed on the left leg. The database also provides maternal R-wave position ($Q\hat{R}S_m$) from AECG and fetal R-wave position ($Q\hat{R}S_f$) from DFECG [22]. If the R waves annotations are not available, an algorithm developed by the authors of the database can be employed [22]. The recordings were digitized with 16-bit resolution at 1000 Hz sampling frequency for DFECG and 500 Hz for AECG.

3.2. Preprocessing

AECG was resampled with a FIR antialiasing low-pass filter (Kaiser window method) at a frequency of 1 kHz [24]. We preprocessed AECG and DFECG with low-pass and high-pass 5th order Butterworth bidirectional filters with 0.5 and 70 Hz cut-off frequencies, respectively. We selected this frequency bandwidth to suppress low-frequency noise and include the spectral energy of interest [25]. Furthermore, 5th order IIR notch bidirectional filter was applied to minimize the power-line interference. We also removed the baseline for all signals using two cascaded median filters, one of 200 samples length and other of 600 samples length. The resulting signal is the baseline and, this is subtracted from the original signal [26, 27]. We can observed this process in Fig 2, Panel A.

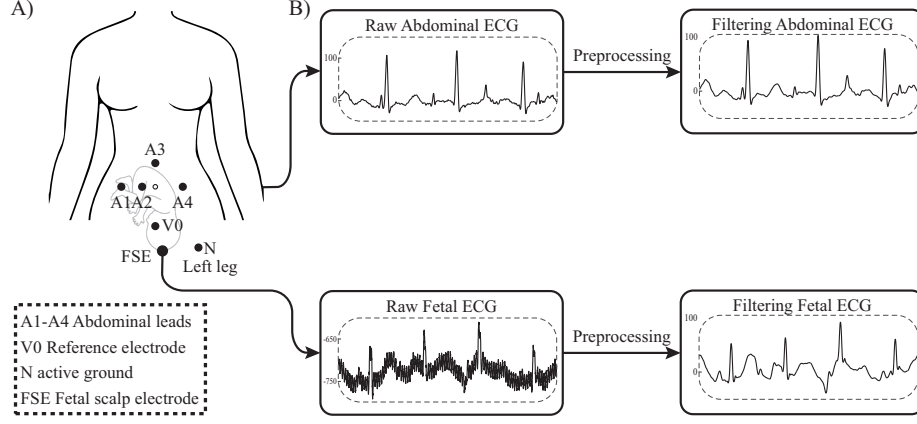


Figure 1: Figure A: Electrode positions used in the ADFECGDB database [22, 23]. Figure B: Representation of the abdominal and fetal ECG signals before and after the filtering described in the "Preprocessing" section.

3.3. QRS complexes discrimination algorithm

We applied the following rule to obtain a sequence of fetal beats with minimal maternal signal interference, (see Fig. 2 Panel B).

$$Q\hat{R}S_{m_i} + 40\%RRf_j + 60ms < Q\hat{R}S_{f_j} < Q\hat{R}S_{m_{i+1}} - 65\%RRf_j - 60ms \quad (1)$$

where $Q\hat{R}S_m$ and $Q\hat{R}S_f$ are maternal and fetal R-wave position, respectively, being RRf_j the time duration between two consecutive fetal beats (Eq. 2) and 60 ms the half of QRS complex duration in the adult [25]. The percentages used in Eq. 1 were determined based on the duration of the fetal cardiac waves, as reported in Pérez et al. [28], such as PR interval, QRS complex, and fetal QT interval durations. Additionally, the algorithm selected a set of N $Q\hat{R}S_f$ for each fetus.

3.4. Beats selection algorithm

The discriminated beats (See Fig. 2 Panel B) must comply with the following criteria: 1) Correlation higher than 0.95 among all fetal QRS complexes; 2) The RR interval duration of the fetal beats (RRf_j) must be within $\pm 5\%$ of the median fetal RR interval ($\overline{RR}f$) (Eq.3). Fig. 2 Panel C shows the aforementioned procedure over the set of N selected $Q\hat{R}S_f$, then:

$$RRf_j = Q\hat{R}S_{f_{j+1}} - Q\hat{R}S_{f_j} \quad (2)$$

$$\overline{RR}f - 5\%\overline{RR}f \leq RRf_j \leq \overline{RR}f + 5\%\overline{RR}f \quad (3)$$

We calculated the correlation between each n^{th} fetal QRS window ($Q\hat{R}S_{f_n} \pm 60$ ms) and the rest of the $N - 1$ QRS windows completing a square $N \times N$ correlation

matrix. For the correlation between each pair, we searched for better possible displacements within the ± 10 samples (± 10 ms) with respect to the original mark in order to correct possible delineation errors, saving the value of the point of the maximum correlation coefficient. For each row, all the elements of the correlation are added together and the row with the highest sum element is then evaluated. Each correlation coefficient in that row is sorted in descending order. Then, the median RR-interval (\widehat{RR}_f) was calculated for this row of N beats to satisfy the second condition. Later, we selected the first 20 QRS complexes that comply with Eq. 3 and also present a correlation greater than 0.95. In cardiology practice, the average of 10 beats is usually taken to generate a template. In this sense, taking into account the noise present in the abdominal signal, it was decided to use 20 beats for the averaging. Fig. 2, Panel C: "Beats selection algorithm" shows the aforementioned procedure over the set of N discriminated $Q\widehat{R}Sf$.

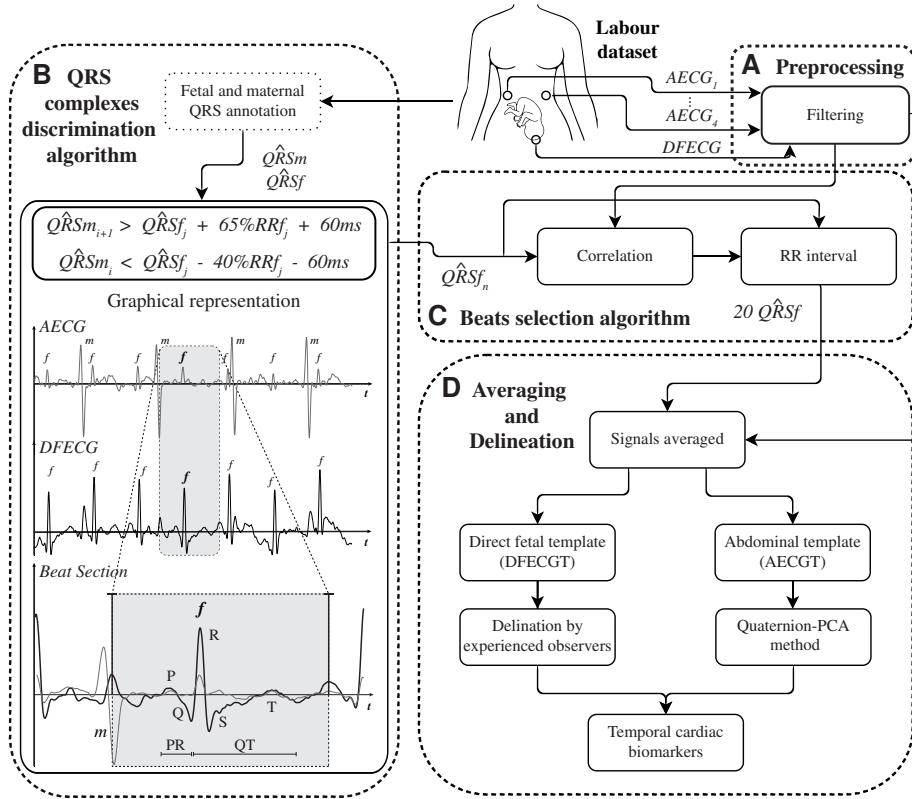


Figure 2: Diagram of the proposed work. **Panel A** corresponds to the preprocessing stage. **Panel B** represents the discrimination of fetal beats using fetal and maternal QRS fiducial points provided by the dataset. As a result of this process, we compute a set of N fetal fiducial points ($Q\widehat{R}Sf_n$). The image shows an illustrative example of fetal beat discrimination. **Panel C**: We evaluate the correlation (≥ 0.95) and stability in the RR interval (Eq. 3) of the selected N beats in Panel B. **Panel D** presents the computing of AECGT and DFECGT from 20 selected fetal beats, and then the obtaining of fiducial points by the Quaternion-PCA method and by experienced observers (*Obs* method), respectively.

3.5. Averaging and Delineating

We constructed the abdominal electrocardiogram templates (AECGT) using 20 beats (subsection 3.4). In addition, DFECG was used as the fetal cardiac signal reference (benchmark) to validate the obtained results, therefore, we also generated high quality DFECG templates (DFECGT). Finally, we used the estimated FHR and other biomarkers [28] to compute the AECGT and DFECGT from the interval defined as:

$$[Q\hat{R}S_f - 200ms : Q\hat{R}S_f + 500ms] \quad (4)$$

We delineated AECGT fiducial points using a novel Quaternion-PCA (Q-PCA) method and also two experienced observers, so called Observer A and Observer B, delineated the DFECGT (see Fig. 2 Panel C: "Delineation"). In this sense, we obtained the following fiducial points: P_{ON} , atrial depolarization onset, QRS_{ON} and QRS_{OFF} , ventricular depolarization onset and end respectively, and T_{END} , ventricular repolarization end, for both, AECGT and DFECGT, respectively.

3.5.1. Q-PCA method

The four abdominal ECG leads provide a mixed of fetal and maternal cardiac electrical information. We calculated the angular velocity of the fetal beats in order to obtain P_{ON} , QRS_{ON} , QRS_{OFF} , and T_{END} . The steps to obtain it are as follows:

Segmentation: To obtain the fiducial points, we used sub-signals from AECGT corresponding to P and T waves and QRS complex. In this way, we considered the following time windows [25] (see Eq. 5, 6, 7 and top and middle panels of Fig. 3).

$$P_{wave} = [1ms : Q\hat{R}S_{f_1} - 80ms] \quad (5)$$

$$QRS_{complex} = [Q\hat{R}S_{f_1} - 60ms : Q\hat{R}S_{f_1} + 60ms] \quad (6)$$

$$T_{wave} = [Q\hat{R}S_{f_1} + 80ms : Q\hat{R}S_{f_2} - 150ms] \quad (7)$$

It is important to highlight that the limits do not indicate the onset or end of the fetal QRS complexes, P or T-wave. They simply demarcate the part of the signal where the waves could be found in the averaged beat.

To reduce the noise and keep the spectral information of each cardiac wave, we applied 10 Hz, 20 Hz and 40 Hz Butterworth low-pass bidirectional filters to sub-signals of T-wave (Eq. 7), P-wave (Eq. 5), and QRS complex (Eq. 6), respectively. We also applied a 0.8 Hz Butterworth high-pass bidirectional filter. This frequency band was selected according to the spectral content of each analyzed cardiac wave [2, 25, 29].

Spatial Analysis:. We used Principal Component Analysis (PCA) to reduce the four abdominal ECG leads to three orthogonal axes. We applied a Singular Value Decomposition to obtain the singular values and vectors of each signal:

$$A = U\Sigma V^T \quad (8)$$

where A represents the P-wave, QRS complex or T-wave sub-signal, U is a 4×4 matrix, V is an $M \times M$ matrix and the four singular values are in the primary diagonal of the $4 \times M$ matrix Σ . The first three elements concentrate the maximum energy, being $A_{\mathbb{S}^3}$ the resulting signal.

Therefore, the decomposed signal Y is:

$$Y_{(4 \times M)} = \Sigma_{(4 \times 4)} V_{(4 \times M)}^T \quad (9)$$

where Σ took the dimensions of 4×4 , since outside of the singular values this matrix is composed of zeros. Conserving the three most significant singular values, we obtained:

$$A_{\mathbb{S}^3} = Y_{(3 \times M)} \quad (10)$$

Cardiac vector velocity:. We consider $A_{\mathbb{S}^3}$ as a sequence $A_m = (A1_m, A2_m, A3_m)$, which represents the three orthogonal components of each sub-signal in the space obtained from PCA. We have previously shown that spatial angular velocity, obtained using quaternion algebra, can be used to define the onset and end of ECG waves [19, 20, 21]. Quaternions are hypercomplex numbers that are of great utility in the study of rotations in three-dimensional space. A quaternion is constituted of a single real unit and three imaginary units that are subject to the Hamilton multiplication rule [30]: $i^2 = j^2 = k^2 = ijk = -1$. The efficacy of this tool is evident when compared to traditional methodologies, such as Euler matrices, in regard to uncertainty propagation and computing time [31]. Consequently, we constructed a quaternion sequence q_m for each m^{th} sample of $A_{\mathbb{S}^3}$.

$$q_m = \frac{(0, A1_m, A2_m, A3_m)}{\|A_m\|} \quad (11)$$

Thus, we applied the temporal differentiation of q_m for the numerical solution of Poisson equation [32] to obtain the angular velocity, because its large deflections make it possible to obtain reference points for the onset and end of cardiac waves [20].

$$\frac{\Delta q}{\Delta m} = (q_{m+1} - q_m) * Fs \rightarrow \vec{\omega} = \frac{\Delta q}{\Delta m} \times \bar{q}_m \quad (12)$$

where Fs is the sampling frequency of the cardiac electrical vector, \bar{q}_m is the quaternion conjugate, and ' \times ' symbol represents the Hamilton multiplication rule of quaternions.

As a last step, the onset and end of ECG waves were obtained from 2-norm of angular velocity to the left and right of the wave peak respectively. We applied Hamming windows to obtain P_{PEAK} and T_{PEAK} from $max(\|A_{\mathbb{S}^3}\|_2)$. Then, we computed the fiducial points from angular velocities: P_{ON} was the peak of the angular velocity to the left of P_{PEAK} , QRS_{ON} and QRS_{OFF} were the first and last peaks of the angular

velocity above the noise level. Finally, T_{END} was defined by the peak of the angular velocity to the right of T_{PEAK} [20, 21]. Bottom panel of Fig. 3 shows the angular velocity ($\|\vec{\omega}\|_2$) of the P-wave, the QRS complex, and the T-wave. We indicated the fiducial points corresponding to P_{ON} , QRS_{ON} , QRS_{OFF} and T_{END} with vertical dotted lines in Fig. 3.

3.6. Experienced observers delineation

We only used the DFECG as a benchmark to validate the proposed algorithm, although it is clear that these data will not be available in daily clinical practice. Two experienced observers measure the ECG fiducial points P_{ON} , QRS_{ON} , $Q\hat{R}S_{f_1}$, QRS_{OFF} , T_{END} and $Q\hat{R}S_{f_2}$ (see top and middle panels of Fig. 3) from DFECG using a computer calibrated cursor (OBs method).

3.7. Temporal cardiac biomarkers

We computed temporal cardiac biomarkers, PR interval, QRS complex width, QT and QTc intervals using the fiducial points obtained from Q-PCA method and OBs method, respectively, according to the following equations:

$$\begin{aligned} PR &= QRS_{ON} - P_{ON} \\ QRS &= QRS_{OFF} - QRS_{ON} \\ QT &= T_{END} - QRS_{ON} \\ QTc &= (T_{END} - Q_{ON})/RR_f \end{aligned} \tag{13}$$

Furthermore, the QT interval was corrected using Bazett's formula, given its dependence on heart rate. For QTc obtained by observers, the RR_f value was calculated using the previously averaged $Q\hat{R}S_{f_1}$ and $Q\hat{R}S_{f_2}$ fiducial points (see Fig. 3). For QTc obtained by the Q-PCA method, we averaged the RR-interval value of the 20 fetal beats selected in "Beats selection algorithm" section.

3.8. Measurements comparison

A Bland-Altman plot is a graphical tool for comparing two measurement techniques [33]. The plot shows the mean of the two measurements in the x-axis, and the difference between the two measurements in the y-axis. The mean of the differences (bias) and the standard deviation of the differences are used to define the limits of agreement. To evaluate the normality of differences, we used the Shapiro-Wilk Normality Test [34] with a p-value ≤ 0.05 .

The Bland-Altman plot and correlation were used to assess interobserver reliability between the two experienced observers and also used to compare the results between Q-PCA method and OBs method using the mean of the interobserver fiducial points, so called \overline{Obs} method.

4. Results

We analyzed 48 AECG templates (12 fetuses \times 4 channels) and 12 DFECG templates (12 fetus \times 1 channel). To construct these templates, approximately 1285 multi-channel beats were processed by Eq. 1, with an average of 107 beats per fetus. Finally, 240 beats obtained from Eq. 2 and Eq. 3 were used. The resulting templates were of high quality templates due to the high correlation of $Q\hat{R}S_f$ (≥ 0.98) and required stability of the RR intervals. As a representative example, Fig. 3 shows the averaged DFECG (top panel) and the averaged AECG (middle panel). Additionally, fiducial points identified by Observer A and Observer B are indicated on the DFECG by circle and square markers. The temporal positions of the angular velocity maximums are shown in the Bottom Panel of Fig 3.

Table 1: Comparative table of temporal cardiac biomarkers obtained with Q-PCA method and experienced observers delineation (*Obs* method).

Fetus	PR [ms]		QRS [ms]		QT [ms]		QTc [ms]	
	Q-PCA	\overline{Obs}	Q-PCA	\overline{Obs}	Q-PCA	\overline{Obs}	Q-PCA	\overline{Obs}
#1	135.0	134.5	70.0	71.0	236.0	245.0	345.0	357.9
#2	103.0	88.5	71.0	79.0	278.0	291.5	414.4	434.5
#3	140.0	126.5	66.0	71.5	205.0	241.0	337.5	397.0
#4	112.0	93.0	79.0	80.5	259.0	292.0	389.1	439.2
#5	141.0	133.0	70.0	71.5	264.0	247.0	384.7	359.7
#6	110.0	93.0	78.0	79.0	268.0	290.5	404.0	437.5
#7	118.0	110.5	75.0	77.5	308.0	311.5	446.9	451.7
#8	150.0	139.0	73.0	72.0	258.0	259.0	378.3	379.8
#9	89.0	85.5	80.0	80.0	269.0	298.5	406.5	450.5
#10	114.0	105.5	69.0	78.0	303.0	304.0	439.2	440.6
#11	145.0	137.0	70.0	70.5	235.0	243.0	343.5	355.2
#12	144.0	138.0	75.0	73.0	250.0	246.5	370.6	365.0
Mean	125.1	115.3	73.0	75.3	261.1	272.5	388.3	405.7
\pmSD	± 19.8	± 21.5	± 4.4	± 4.0	± 28.5	± 27.6	± 35.9	± 40.1
Correlation	0.97		0.67		0.84		0.79	
p-value	$< 2.39e - 7$		$< 1.74e - 2$		$< 7.05e - 4$		$< 2.27e - 3$	

Table 1 presents fetal cardiac biomarkers computed by the Q-PCA method and the *Obs* method. The RR-interval values used to compute QTc interval for Q-PCA and *Obs* methods were 451.5 ± 29.3 ms and 451.8 ± 29.5 ms, respectively (expressed as mean \pm SD over 12 fetuses). In addition, the correlation between the two methods for the values PR interval, QRS interval, QT and QTc intervals were: 0.97, 0.67, 0.84, and 0.79, respectively.

We have used a reliable signal of fetal cardiac electrical activity, i.e. the DFECG signal. This signal is not disturbed by the maternal ECG signal and therefore the manual measurements on it are used as a benchmark. To obtain the values for the *Obs* method, we first analyzed the concordance of the fiducial points defined by each observer using Bland-Altman plots. The distribution of the differences of fiducial points

between observers exhibited a normal distribution, with the exception of QRS_{OFF} , which did not meet the normality condition. Therefore, in the latter case, the Bland-Altman plot was analyzed using non-parametric methods, where the median was used as the bias and the 2.5 and 97.5 percentiles as the limits of agreement [35], as shown in Fig. 4. The QRS_{ON} and QRS_{OFF} fiducial points showed minimal dispersion between observers, with mean differences close to 0.5 ms. However, the P_{ON} and T_{END} markers exhibited greater dispersion. The P_{ON} analysis revealed that two fetuses (#6 and #10) has differences exceeding the accepted limits, with discrepancies of 6 and 3.73 ms respectively, while there are three cases of complete agreement between observers. In contrast, only one fetus (#4) fell outside the T_{END} limits, showing a discrepancy of 28 ms between observers. In this case, the baseline was not clearly defined, which could have resulted in variations in the observers criteria. In addition, fetuses #10 and #11 also showed a difference of 23 and 14 ms, respectively. Similarly, we observed high correlation levels between observers for P_{ON} : 0.99 ($p < 8.46e - 6$), QRS_{ON} : 0.94 ($p < 7.80e - 6$), QRS_{OFF} : 0.98 ($p < 1.42e - 8$), and T_{END} : 0.93 ($p < 8.46e - 6$). As we can observe in Fig. 5, the Bland-Altman plots demonstrated the agreement between the Q-PCA and Obs methods.

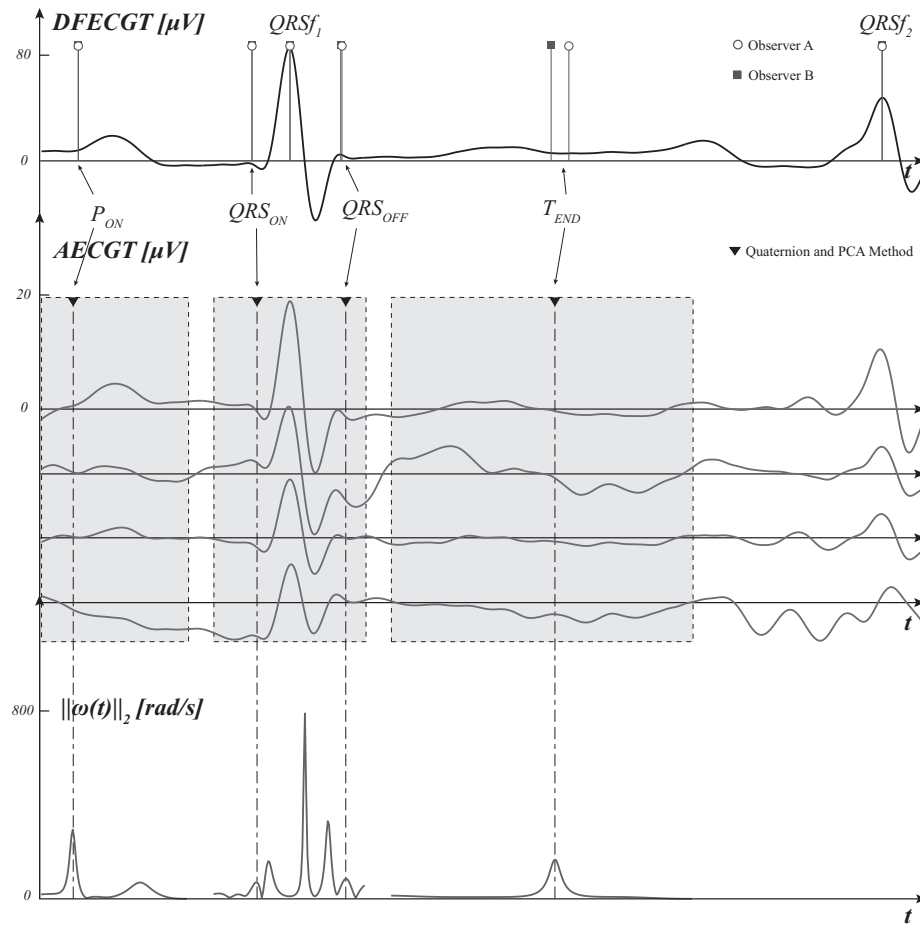


Figure 3: **Top panel:** DFECGT delineation measured by Observer A and Observer B (circle and square marks). **Middle panel:** AECGT delineation using Q-PCA method. The shaded area corresponds to the time windows defined in section 3.5 Averaging and Delineation, subsection Q-PCA method, i.e., P-wave, QRS complex, and T-wave sub-signals. **Bottom panel:** Angular velocity signal. The position of the onset and end of these waves are represented with vertical dotted lines ending in triangular marks.

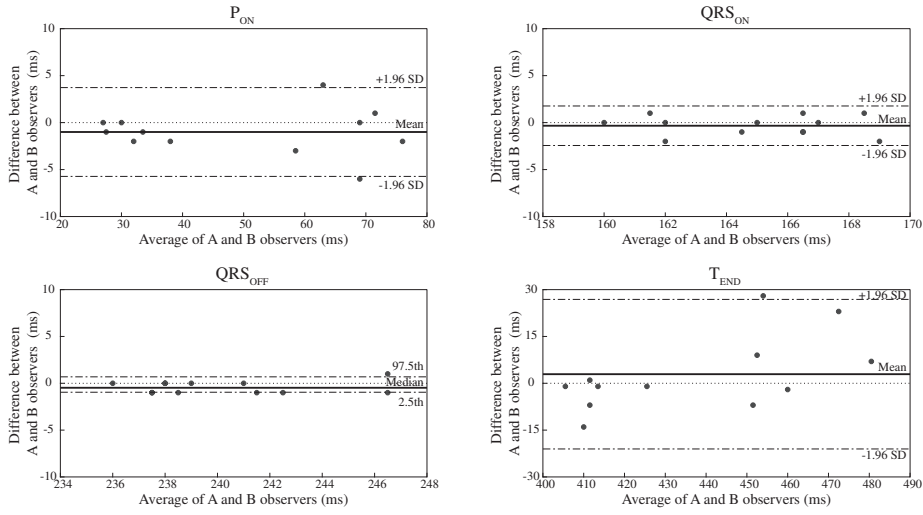


Figure 4: Bland-Altman plot comparing the fiducial points of P_{ON} , QRS_{ON} , QRS_{OFF} , T_{END} as calculated by Observer A and Observer B. The plot shows the bias of measurement with a black line and the limits of agreement with CI 95% in discontinued line. The bias found for each fiducial point was: P_{ON} : -1 ms (CI: $-5.73 - 3.73$), QRS_{ON} : -0.33 ms (CI: $-5.06 - 4.39$), QRS_{OFF} : -0.5 ms (CI: $-1 - 0.73$) and T_{END} : 2.92 ms (CI: $-1.81 - 7.64$). The maximum standard deviation occurs at the end of the T-wave, while the minimum occurs at the end of the QRS complex.

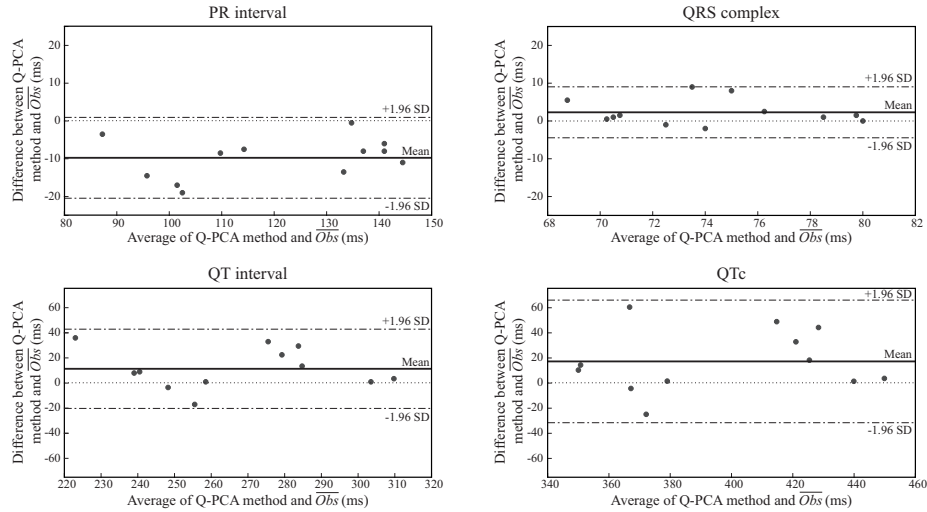


Figure 5: Bland-Altman plot comparing the fetal cardiac biomarkers obtained by the Q-PCA method and \overline{Obs} method. The plot shows the bias of measurement with a black line and the limits of agreement with CI 95% in discontinued line. The bias found for each cardiac biomarker was: PR interval: -9.75 ms (CI: $-20.45 - 0.95$), QRS duration: 2.29 (CI: $-4.45 - 9.04$), QT interval: 11.38 (CI: $-20.18 - 42.93$) and QTc: 17.26 (CI: $-31.56 - 66.08$) It is important to note that the dispersion of QT and QTc measurements is also related to the dispersion already observed between observers at T-wave end, as well as to the characteristics of each fetus.

5. Discussion

During fetal growth or labor, a NIFECG can be used to evaluate cardiac health [6, 12]. The main objective of this work was to implement a simple processing method of the non-invasive fetal ECG to calculate cardiac biomarkers as faithfully as possible with the highest possible accuracy. An algorithm was implemented to discriminate and select fetal QRS annotations from maternal QRS annotations, thus preventing the maternal signal from influencing the obtained fetal beat template. As the focus of this study is not on detecting these fiducial points, if fiducial points are unavailable, alternative algorithms, such as the one proposed by Agostinelli et al. [36], can be applied.

According to Fig. 5, the largest difference between \overline{Obs} and Q-PCA methods was observed in QT and QTc intervals. However, the bias for QT and QTC is within 5% of the duration obtained with the Q-PCA method. In the same way that Martinek et al. [37], we obtained the most significant discrepancy in fetus #3 (36 ms and 59.3 ms for QT and QTc intervals, respectively), likely caused by the low signal-to-noise ratio (SNR) in this recording [23]. We assumed these differences could be attributed to the uncertainty in defining the T-wave end. With regard to the PR interval, it is the parameter that demonstrates the greatest dispersion in relation to the mean value obtained by the Q-PCA method. Moreover, the QRS duration differences did not exceed more than 2 ms of in 67% of cases, further supporting the hypothesis that the T-wave end definition poses the main challenge.

Taking into account similar stages of pregnancy, we compared our results with those published by other authors, see Table 2. We found similar results to PR interval of Taylor et al.[38], this author did not present the mean \pm SD. However, we found differences of about 7 to 15 ms with the other authors [9, 10, 11]. This difference could be attributed to averaging, i.e. distortions in the onset of the P-wave could be due to the influence of the maternal T-wave. In adults, parasympathetic changes and severe hypoxia have been shown to prolong the PR interval [39]. Whereas in intrapartum fetal monitoring, it can be used to determine fetal acidosis [40]. Moreover, the PR interval is an electrocardiographic parameter to diagnose fetal asphyxia [1].

Table 2: Comparative table of temporal cardiac biomarkers obtained by others authors (mean \pm SD). *Prediction values of biomarkers by linear regression with CI 95%.

Author	PR [ms]	QRS [ms]	QT [ms]	QTc [ms]
Chivers et al.[11] (GA: 20-40 weeks)	118.54 \pm 23.21	58.34 \pm 5.73	261.63 \pm 36.16	396.40 \pm 45.78
Wacker-Gussman et al.[10] (GA: 39 weeks)	113 \pm 16	50 \pm 6	241 \pm 26	367 \pm 32
Chia et al.[9] (GA: \geq 37 weeks)	110.1 \pm 9.4	52.6 \pm 7.4	242.7 \pm 16.1	367.7 \pm 28.5
Taylor et al.[38] (GA: 38-42 weeks)	86 – 141	47 – 69	233 – 329	292 – 491
Taylor et al.*[8] (GA: 40 weeks)	105.16 (80.2 – 137.8)	54.6 (41.0 – 72.8)	258.88 (204.3 – 313.5)	392.8 (308.20 – 392.8)
This work (GA: 20-40 weeks)	125.1 \pm 19.8	73.0 \pm 4.4	261.1 \pm 28.5	388.3 \pm 35.9

On the other hand, QRS interval has been linked to several pathological conditions such as: indicator of fetal growth restriction (IUGR) [3, 41], hematological disease [42], and basal tachycardia [37]. Our results were comparable with the maximum values obtained by Taylor et al. [38], however, there are significant differences of approximately 20 ms with Wacker-Gussmann et al. [10] and Chia et al. [9] and slightly less (12 ms) with Chivers et al. [11]. In our study, we observed a low bias between the Q-PCA method and the observers for the QRS intervals. The underestimation of QRS width as measured by other authors could be linked to a some degree of uncertainty in the identification of the end of the QRS complex.

The QT interval could be useful for premature diagnosis of intrapartum hypoxia and fetal acidosis [1, 4, 12, 39]. Sato et al. [39] observed prolonged QTc interval in fetuses with nonimmune fetal hydrops, dilated cardiomyopathy, cardiac abnormality, and IUGR. On the other hand, Velayo et al. successfully differentiated healthy fetuses from those with IUGR using QT and QTc intervals [43]. Schwartz et al. [44] found a strong association between QT prolongation and sudden infant death syndrome in neonates, with a mean QTc interval of 435 ± 45 ms in those who died, compared to 400 ± 20 ms in survivors. Using the Q-PCA method, the QT and QTc intervals obtained were found to be closely matched to the results previously reported by Wacker-Gussmann et al. [10], Chia et al. [9] and Chivers et al. [11]. The maximum observed discrepancy was approximately 20 milliseconds, which is less than the standard deviation reported by the authors. The difference found in the results for the end of the T-wave may have also been transferred to obtain the QT and QTc intervals. These discrepancies, particularly at the T_{END} point, see Fig. 4, align with observations by other researchers regarding the complexity of T-wave morphology [9, 10]. In the case of Taylor et al. [38], the results obtained with the Q-PCA method are within the range presented by the author.

Also, Taylor et al. [8] predicted fetal cardiac interval durations through linear regression. The PR interval and QT and QTc intervals obtained by the Q-PCA method were within the confidence interval provided in the study (Table 2). In the case of QRS complex width, it exceeded the maximum interval value by less than 1 ms. In all cases, the values found were closer to the upper limit of the confidence interval.

6. Study limitations

The algorithm has been evaluated for gestational stages close to labour, as our results have been validated using the DFECG. It has been applied to healthy patients, so it cannot be assumed that it will be effective when applied to fetuses with any pathology.

It should be noted that the abdominal signals recorded by the different authors and those in this study were recorded with different configurations and numbers of electrodes. In order to obtain fetal cardiac parameters in the future, it is essential to standardize the recording of abdominal signals and generate a new database with a larger number of patients.

7. Conclusions

In this work, we have obtained fetal cardiac biomarkers using a non-invasive fetal monitoring technique. We developed an algorithm capable of detecting fetal beats

with low maternal ECG influence. This algorithm generated high quality fetal beat templates that allowed us to achieve very good delineation performance using the Q-PCA method. Considering the fact that there are no standard values of fetal cardiac waves, promising results were obtained based on our method. As diagnosis using fetal electrocardiograms is not yet routine in clinical practice, and given its importance, it is necessary to further develop these techniques with the aim of developing non-invasive fetal health monitoring devices.

References

- [1] Abel JD, Dhanalakshmi S, Kumar R. A comprehensive survey on signal processing and machine learning techniques for non-invasive fetal ECG extraction. *Multimed Tools Appl.* 2022;82:1373–1400.
- [2] Sameni R, Clifford GD. A Review of Fetal ECG Signal Processing Issues and Promising Directions. *Electrophysiology and Therapy Journal.* 2010;3:4-20.
- [3] Agostinelli A, Grillo M, Biagini A, Giuliani C, Burattini L, Fioretti S, et al. Non-invasive Fetal Electrocardiography: An Overview of the Signal Electrophysiological Meaning, Recording Procedures, and Processing. *Ann Noninvasive Electrocardiol.* 2015;20(4):303–313.
- [4] Kahankova R, Martinek R, Jaros R, Behbehani K, Matonia A, Jezewski M, et al. A Review of Signal Processing Techniques for Non-Invasive Fetal Electrocardiography. *IEEE Reviews in Biomedical Engineering.* 2020;13:51-73.
- [5] Pegorie C, Liu B, Thilaganathan B, Bhide A. Antenatal Noninvasive Fetal Electrocardiography: A Literature Review. *Maternal-Fetal Medicine.* 2024;6(3):178-89.
- [6] Hasan MA, Reaz MBI, Ibrahimy MI, Hussain MS, Uddin J. Detection and Processing Techniques of FECG Signal for Fetal Monitoring. *Biological Procedures Online.* 2009;11(1):263-95.
- [7] Alshebly YS, Nafea M. Isolation of Fetal ECG Signals from Abdominal ECG Using Wavelet Analysis. *IRBM.* 2019.
- [8] Taylor MJO, Smith MJ, Thomas MJ, Green AR, Cheng F, Oseku-Afful S, et al. Non-invasive fetal electrocardiography in singleton and multiple pregnancies. *International Journal of Obstetrics and Gynaecology.* 2003;110:668-78.
- [9] Chia EL, Ho TF, Rauff M, Yip WCL. Cardiac time intervals of normal fetuses using noninvasive fetal electrocardiography. *Prenatal Diagnosis.* 2005;25:546-52.
- [10] Wacker-Gussmann A, Plankl C, Sawald M, Schneider KM, Oberhoffer R, Lobmaier SM. Fetal cardiac time intervals in healthy pregnancies - an observational study by fetal ECG (Monica Healthcare System). *J Perinat Med.* 2018;46(6):587-92.

- [11] Chivers SC, Vasavan T, Nandi M, Hayes-Gill BR, Jayawardane IA, Simpson JM, et al. Measurement of the cardiac time intervals of the fetal ECG utilising a computerised algorithm: A retrospective observational study. *JRSM Cardiovascular Disease*. 2022;11:1-11.
- [12] Behar JA. Extraction of Clinical Information from the Non-Invasive Fetal Electrocardiogram [PhD thesis]. University of Oxford; 2014.
- [13] Lakhno I, Behar JA, Oster J, Shulgin V, Ostras O, Andreotti F. The use of non-invasive fetal electrocardiography in diagnosing seconddegree fetal atrioventricular block. *Maternal Health, Neonatology, and Perinatology*. 2017;3(14).
- [14] Behar JA, Bonnemains L, Shulgin V, Oster J, Oleksii Ostras O, Lakhno I. Non-invasive fetal electrocardiography for the detection of fetal arrhythmias. *Prenatal Diagnosis*. 2019;39:178–187.
- [15] Hayashi R, Nakai K, Fukushima A, Itoh M, Sugiyama T. Development and Significance of a Fetal Electrocardiogram Recorded by Signal-Average High-Amplification Electrocardiography. *Int Heart J*. 2009;50(2):161-71.
- [16] Marcantoni I, Vagni M, Agostinelli A, Sbrollini A, Morettini M, Burattini L, et al. T-Wave Alternans Identification in Direct Fetal Electrocardiography. *Computing in Cardiology*. 2017;44:1-4.
- [17] Marcantoni I, Sbrollini A, Burattini L, Morettini M, Fioretti S, Burattini L. Automatic T-Wave Alternans Identification in Indirect and Direct Fetal Electrocardiography. 40th Annual International Conference of the IEEE Engineering in Medicine and Biology Society (EMBC). 2018:4852-5.
- [18] Yilmaz B, Narayan HK, Wilpers A, Wiess C, Fifer WP, Williams IA. Electrocardiographic Intervals in Fetuses with Congenital Heart Disease. *Cardiology in the Young*. 2016;26(1):84-9.
- [19] Cruces PD, Arini PD. Quaternion-based study of angular velocity of the cardiac vector during myocardial ischaemia. *Int J Cardiol*. 2017;248:57-63.
- [20] Cruces PD, Torkar D, Arini PD. Dynamic features of cardiac vector as alternative markers of drug-induced spatial dispersion. *Journal of Pharmacological and Toxicological Methods*. 2020;104:1-8.
- [21] Cruces PD, Toscano A, Alvarado Rodríguez FJ, Romo-Vázquez R, Arini PD. Drug-induced symmetry effects on ventricular repolarization dynamics. *Biomed Signal Proc and Control*. 2023;81:104493.
- [22] Jezewski J, Matonia A, Kupka T, Jezewski M, Roj D, Czabanski R. Determination of fetal heart rate from abdominal signals: evaluation of beat-to-beat accuracy in relation to the direct fetal electrocardiogram. *Biomed Tech*. 2012;57(5):383-894.
- [23] Matonia A, Jezewski J, Kupka T, Jezewski M, Horoba K, Wrobel J, et al. Fetal electrocardiograms, direct and abdominal with reference heartbeat annotations. *Sci Data*. 2020;7(200).

- [24] The MathWorks, Inc . Signal Processing Toolbox R2020a; 2020. Version 9.9.0. <https://www.mathworks.com>.
- [25] Sörnmo L, Laguna P. Bioelectrical Signal Processing in Cardiac and Neurological Applications. Elsevier Inc.; 2005.
- [26] de Chazal P, O'Dwyer M, Reilly RB. Automatic Classification of Heartbeats Using ECG Morphology and Heartbeat Interval Features. IEEE Transactions on Biomedical Engineering. 2004;51(7):1196-206.
- [27] Marianux. ECG-kit; 2025. Downloaded 29 January, 2025. Available from: <https://github.com/marianux/ecg-kit>.
- [28] Pérez FJ, Picarzo L. Guía rápida para la lectura sistemática del ECG Pediátrico. Rev Pediatr Aten Primaria. 2006;8(3):19-26.
- [29] Tompkins WJ. Biomedical Digital Signal Processing: C Language Examples and Laboratory Experiments for the IBM PC. Prentice Hall; 2000.
- [30] Meister L, Schaeben H. A concise quaternion geometry of rotations. Mathematical Methods in the Applied Sciences. 2005;28:101-26.
- [31] Barsky BA, editor. Rethinking Quaternions. Theory and Computation. Morgan & Claypool, California; 2010.
- [32] Poznyak AS. 2. In: Modelado Matemático de los Sistemas Mecánicos, Eléctricos y Electromecánicos. Pearson; 2005. p. 73-83.
- [33] Bland JM, Altman DG. Statistical methods for assessing agreement between two methods of clinical measurement. The Lancet. 1986;1(8476):307-10.
- [34] Shapiro SS, Wilk MB. An analysis of variance test for normality (complete samples). Biometrika. 1965;52(3-4):591-611.
- [35] Bland JM, Altman DG. Measuring agreement in method comparison studies. Statistical Methods in Medical Research. 1999;8:135-60.
- [36] Agostinelli A, Marcantoni I, Moretti E, Sbröllini A, Fioretti S, Di Nardo F, et al. Noninvasive Fetal Electrocardiography Part I: Pan-Tompkins' Algorithm Adaptation to Fetal R-peak Identification. The Open Biomedical Engineering Journal. 2017;11:17-24.
- [37] Martinek R, Kahankova R, Jaros R, Barnova K, Matonia A, Jezewski M, et al. Non-Invasive Fetal Electrocardiogram Extraction Based on Novel Hybrid Method for Intrapartum ST Segment Analysis. IEEE Access. 2021;9:28608-31.
- [38] Taylor MJO, Thomas MJ, Smith MJ, Oseku-Afful S, Fisk NM, Green AR, et al. Non-invasive intrapartum fetal ECG: preliminary report. International Journal of Obstetrics and Gynaecology. 2005;112:1016-21.

- [39] Sato N, Hoshiai T, Ito T, Owada K, Chisaka H, Aoyagi A, et al. Successful Detection of the Fetal Electrocardiogram Waveform Changes during Various State of Singletons. *Tohoku J Exp Med.* 2011;225(2):89-94.
- [40] Reed NN, Mohajer MP, Sahota DS, James DK, Symonds EM. The potential impact of PR interval analysis of the fetal electrocardiogram (FECG) on intrapartum fetal monitoring. *European Journal of Obstetrics, Gynecology, and Reproductive Biology.* 1996;68(1):87–92.
- [41] Smith V, Arunthavanathan S, Nair A, Ansermet D, da Silva Costa F, Wallace EM. A systematic review of cardiac time intervals utilising non-invasive fetal electrocardiogram in normal fetuses. *BMC Pregnancy and Childbirth.* 2018;18(1):370.
- [42] Brabati B, Pardi G. The intraventricular conduction time of fetal heart in pregnancies complicated by rhesus haemolytic disease. *British Journal of Obstetrics and Gynaecology.* 1981;88:1233-40.
- [43] Velayo CL, Funamoto K, Silao JNI, Kimura Y, Nicolaides K. Evaluation of Abdominal Fetal Electrocardiography in Early Intrauterine Growth Restriction. *Front Physiol.* 2017;8:437.
- [44] Schwartz PJ, Stramba-Badiale M, Segantini A, Austoni P, Bosi G, Giorgetti R, et al. Prolongation of the QT interval and the sudden infant death syndrome. *The New England Journal of Medicine.* 1998;338(24):1709-14.

8. Statements & Declarations

8.1. Acknowledgment

This work was supported by CONICET under project [PUE-22920170100026], Argentina. In addition, grants [PICT 2020-SERIEA-00457] by National Agency for the Promotion of Research, Technological Development and Innovation and [PIP 11220210100284CO] by CONICET, Argentina.

8.2. Competing Interests

The authors have no relevant financial or non-financial interests to disclose.

8.3. Ethical Approval

Not Applicable.

8.4. Consent to Participate

Not Applicable.

8.5. Consent to Publish

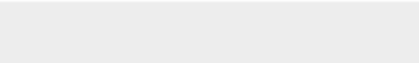
Not Applicable.



Click here to access/download
LaTeX Source File
refs.bib



Click here to access/download
LaTeX Source File
Elsevier_IRBM.tex



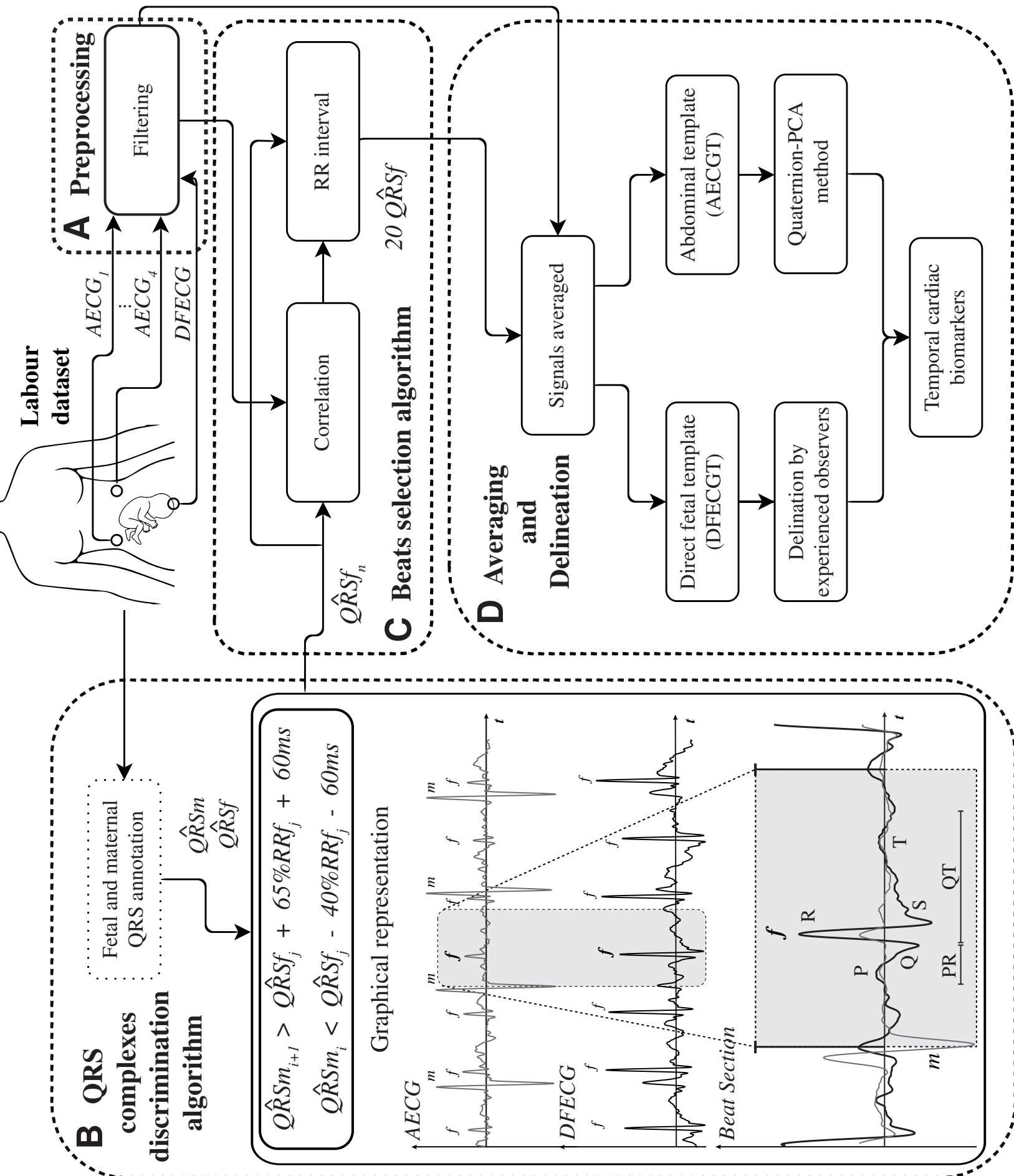


Figure 2

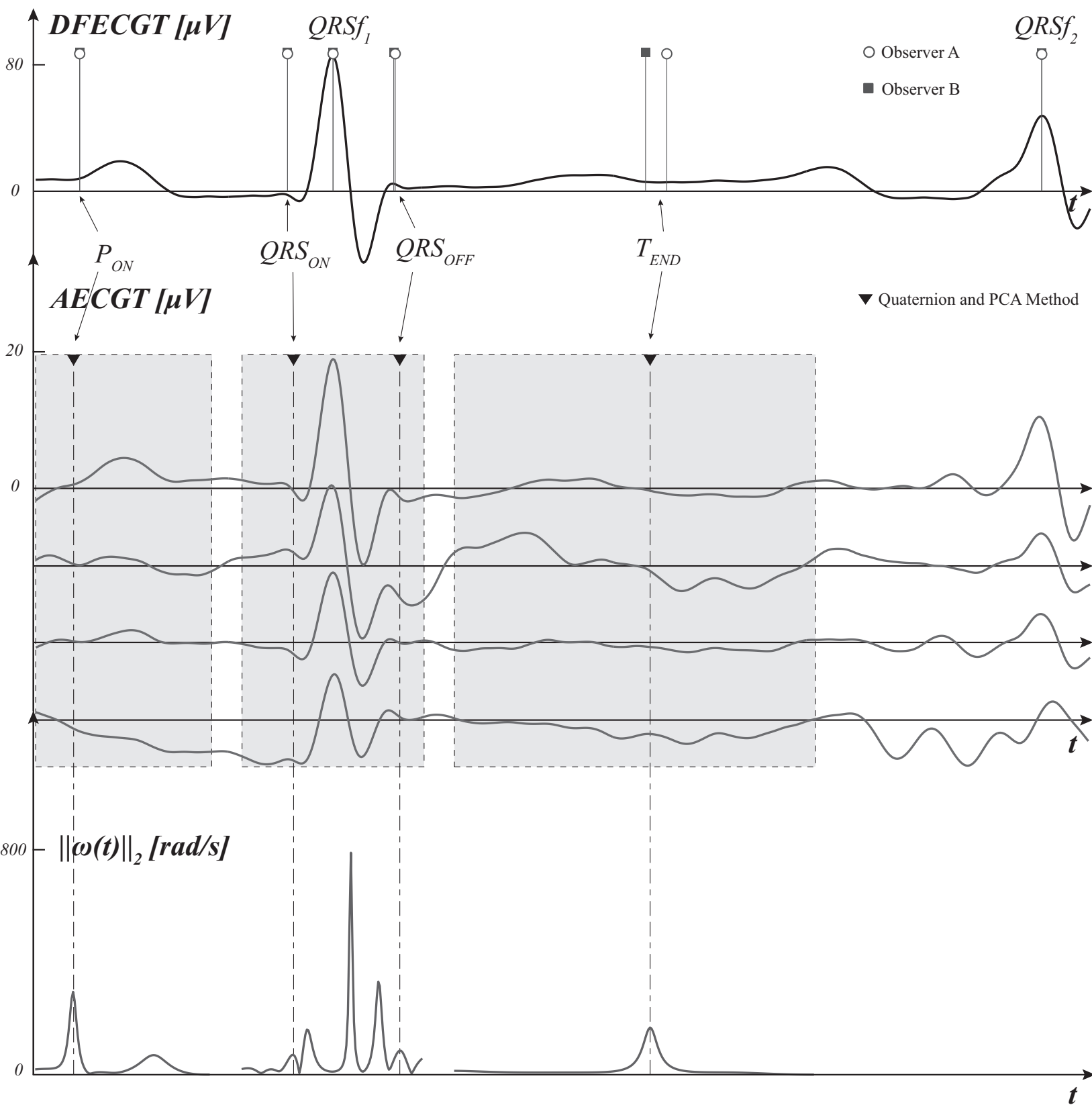


Figure 3

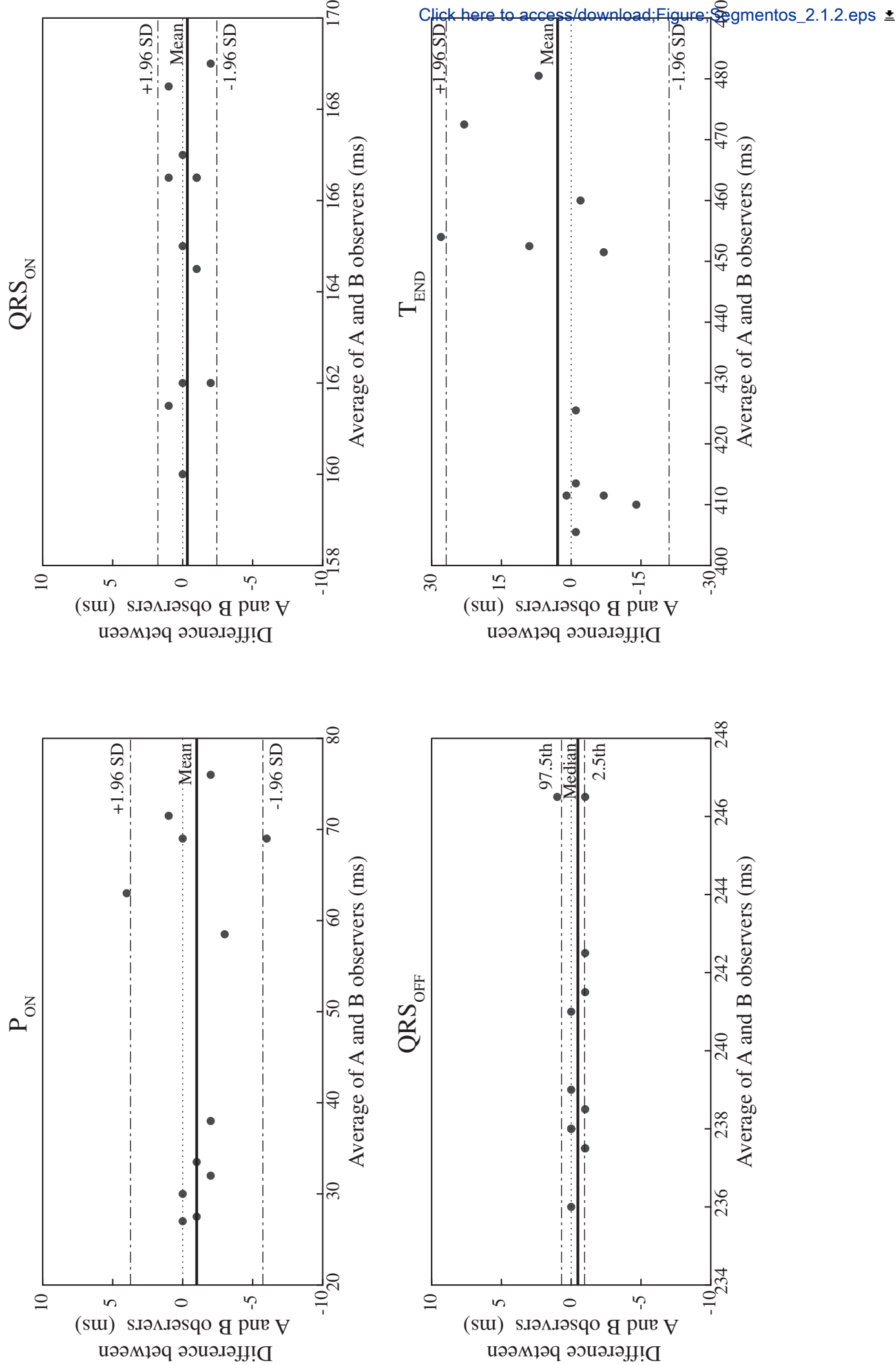
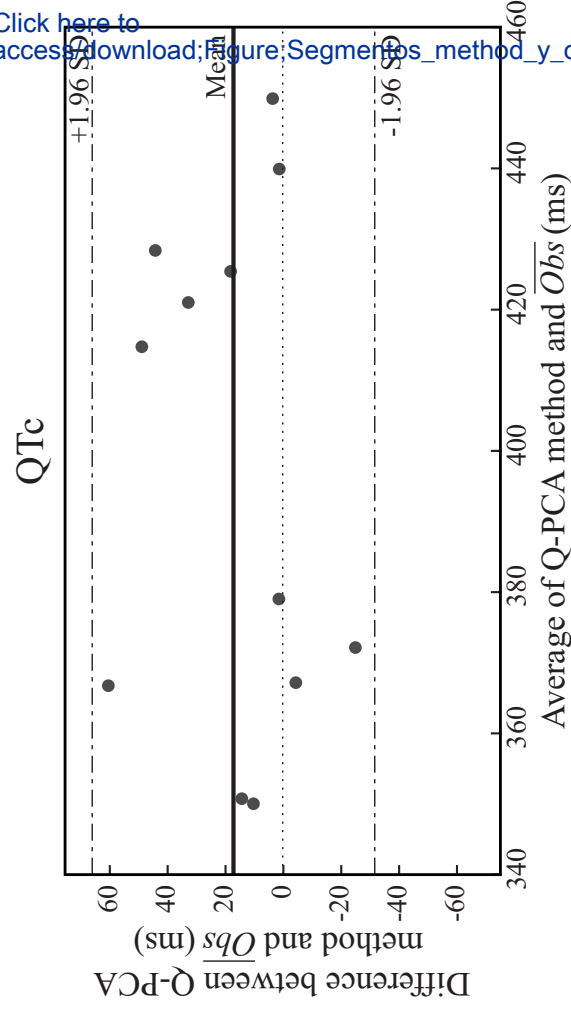
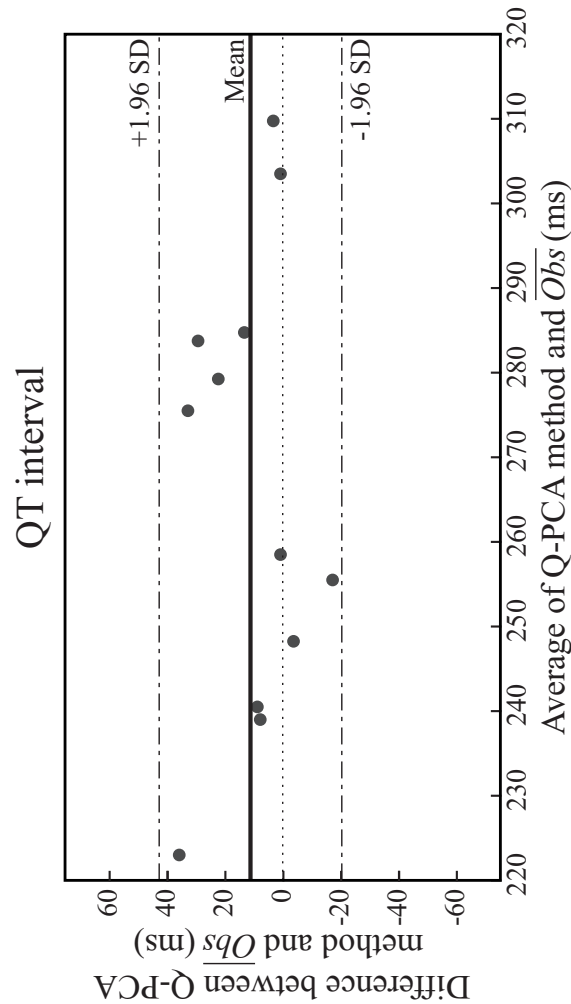
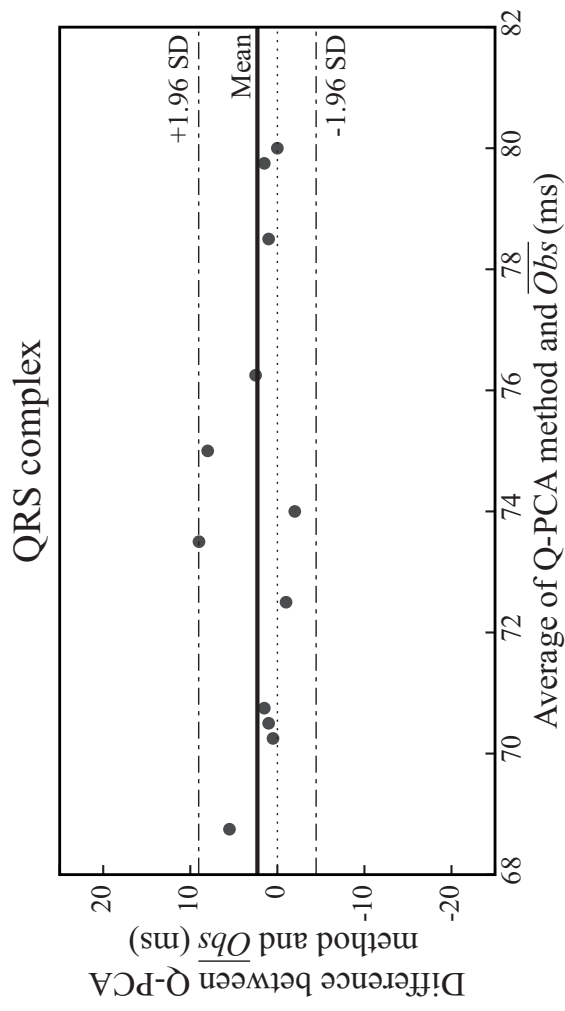
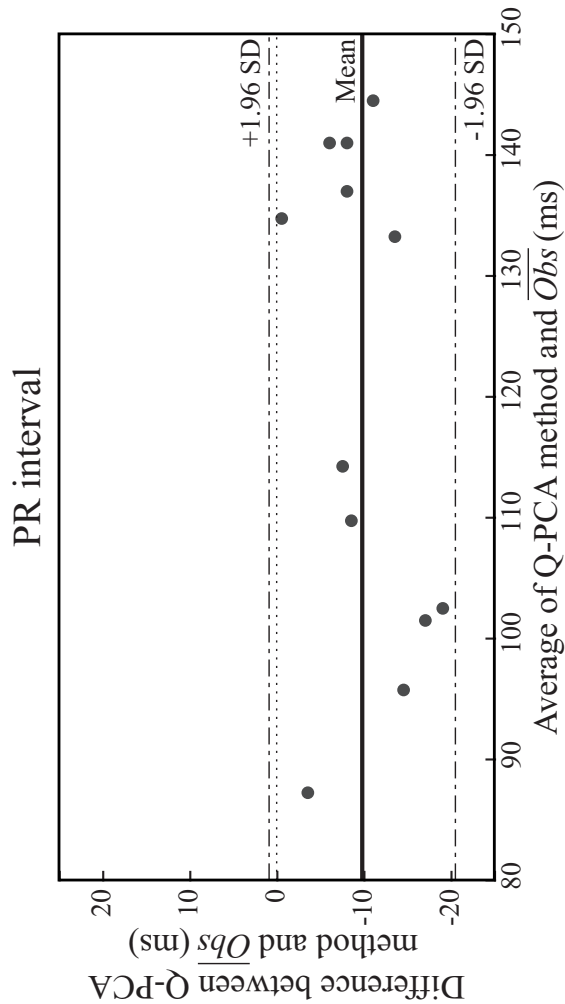


Figure 4



[Click here to access/download;Figure_Segments_method_y_obs.eps](#)

Figure 5

[Click here to access/download;Figure;grafica_signals.eps](#)

